Available online at www.sciencedirect.com
SCIENCE DIRECT®
Journal of Organometallic Chemistry 690 (2005) 519–533
Journal of Organometallic Chemistry
www.elsevier.com/locate/jorganchem

Syntheses, crystal structures and coordination modes of tri- and di-organotin derivatives with 2-mercapto-4-methylpyrimidine

Chunlin Ma [a,b,*], Junhong Zhang [a], Guangru Tian [a], Rufen Zhang [a]

[a] Department of Chemistry, Liaocheng University, Liaocheng 252059, People's Republic of China
[b] Taishan University, Taian 271021, People's Republic of China

Received 10 August 2004; accepted 5 October 2004

Abstract

The organotin (IV) derivatives of 2-mercapto-4-methylpyrimidine (Hmpymt) R_3SnL (R = Ph **1**, $PhCH_2$ **2**, *n*-Bu **3**), $R_2SnCl_mL_n$ ($m = 1$, $n = 1$, R = CH_3 **4**, Ph **5**, *n*-Bu **6**, $PhCH_2$ **7**; $m = 0$, $n = 2$, R = CH_3 **8**, *n*-Bu **9**, Ph **10**, $PhCH_2$ **11**) were obtained by the reaction of the organotin(IV) chlorides R_3SnCl or R_2SnCl_2 with 2-mercapto-4-methylpyrimidine hydrochloride (HCl · Hmpymt) in 1:1 or 1:2 molar ratio. All complexes **1**–**11** were characterized by elemental analyses, IR, ^1H, ^{13}C and temperature-dependent ^{119}Sn NMR spectra. Except for complexes **3** and **6**, the structures of complexes **1**, **2**, **4**, **5**, **7**, **8**–**11** were confirmed by X–ray crystallography. Including tin-nitrogen intramolecular interaction, the tin atoms of complexes **1**–**7** are all five-coordinated and their geometries are distorted trigonal bipyramidal. While the tin atoms of complexes **8**–**11** are six-coordinated and their geometries are distorted octahedral. Besides, the ligand adopts the different coordination modes to bond to tin atom between the complexes **1**, **6**, **7** and **2**, **3**, **4**, **5**, **8**–**11**. Furthermore, intermolecular Sn···N or Sn···S interactions were recognized in crystal structures of complexes **4**, **7** and **11**, respectively.

Keywords: 2-Mercapto-4-methylpyrimidine; Organotin; Crystal structures

1. Introduction

The coordination chemistry of tin is extensive with various geomertries and coordination numbers known for both inorganic and organometallic complexes [1]. Higher coordination numbers can be generated either by inter- and/or intra-molecular interaction, especially in complexes where tin bonds to electronegative atoms, such as oxygen, nitrogen and sulfur. Studies of adducts of organotin halides continue to provide fundamental information about both the Lewis acid-base model and the reactivity of organotin species [2]. Furthermore, organotin(IV) complexes show a large spectrum of biological activities. In recent years, several investigations to test their antitumour activities have been carried out and much attention has been focused on their antitumour properties and their implications in antioncogenesis [3]. Also, they are used commercially as bactericides, fungicides, acaricides and industrial and agriculture biocides [4,5]. The presence of 2-mercaptopyrimidine nucleotides has been detected in *Escherichia coli* sRNA and yeast tRNA, it was found to inhibit the synthesis of tRNA and thus it acts as an antitumour and antithyroid agent [6]. A similar inhibitory effect has been found for pyrimidine-2-thione (Hpymt) and the compound also shows pronounced *in vitro* bacteriostatic activity [7].

To continue our studies on the coordination of organotin(IV) moieties by thiol sulfur and heterocyclic nitrogen [8–10] we choose another ligand: 2-mercapto-4-methylpyrimidine (Hmpymt), similar to the

* Corresponding author. Tel.: +86 635 8258579; fax: +86 538 6715521.
E-mail address: macl@lctu.edu.cn (C. Ma).

0022-328X/$ - see front matter © 2004 Elsevier B.V. All rights reserved.
doi:10.1016/j.jorganchem.2004.10.020

2-mercaptopyrimidine (Hpymt) and 4,6-dimethylpyrimidine-2-thione (Me_2PymtH) [11], they belong to the same class as the nucleic acid bases. It is worth to note that since the 2-mercapto-4-methylpyrimidine is an unsymmetrical ambidentate ligand, besides, with the cooperation between steric repulsion and interactions [12,13], its N,S-bidentate coordination to the tin atom generates linkage isomerism. As shown in Fig. 1, there is an adjacent isomer with the C^4 methyl group of the pyrimidine ring near the R_n– chelates (**A**) and a remote isomer with the C^4 methyl group distant from the R_n– chelates (**B**). In this paper, we reported the syntheses, crystal and molecular structures of the related organotin derivatives **1**–**11**, which exhibit versatile structures, based upon different coordination modes of Hmpymt (Scheme 1).

All complexes **1**–**11** were characterized by elemental analyses, IR, ^{1}H NMR, ^{13}C NMR and ^{119}Sn NMR spectra. Except for complexes **3** and **6**, complexes **1**, **2**, **4**, **5**, **7**, **8**–**11** have been determined by X-ray crystallography. From the crystal structures, we can see that in complexes **2**, **4**, **5** and **9**–**11**, the ligand adopts mode **B** to bond to tin atom through the 1-nitrogen and 2-sulfur donors, while adopts mode **A** to bond to tin atom through the 3-nitrogen and 2-sulfur donors in complexes **1** and **7**, and not only through the 1-nitrogen and 2-sulfur donors but also through the 3-nitrogen and 2-sulfur donors mode in complex **8**.

2. Experimental

2.1. Materials and measurements

Triphenyltin chloride, tribenzyltin chloride, tributyltin chloride, diphenyltin dichloride, di-*n*-butyltin dichloride, dimethyltin dichloride and 2-mercapto-4-methylpyrimidine hydrochloride (HCl · Hmpymt) were commercially available, and they were used without further purification. Dibenzyltin dichloride were prepared by a standard method reported in the literature [14]. The melting points were obtained with Kofler micro melting point apparatus and were uncorrected. Infrared-spectra were recorded on a Nicolet–460 spectrophotometer using KBr discs and sodium chloride optics. ^{1}H and ^{13}C ^{119}Sn NMR spectra were recorded on a Bruker AMX–300 spectrometer operating at 300 and 75.3, 149.2 MHz, respectively. The ^{1}H and ^{13}C spectra were acquired at room temperature (298 K) and ^{119}Sn NMR were obtained at different temperature unless otherwise specified; ^{13}C spectra are broadband proton decoupled. The chemical shifts were reported in ppm with respect to the references and were stated relative to external tetramethylsilane (TMS) for ^{1}H, ^{13}C NMR, and to neat tetramethyltin for ^{119}Sn NMR. Elemental analyses were performed with a PE–2400II apparatus.

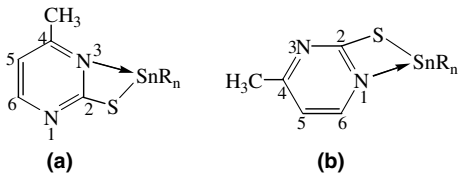

Fig. 1. (a) Adjacent; (b) remote.

2.2. Synthesis

The general route of synthesis is shown in the following. The reaction was carried out under nitrogen atmosphere with use of standard Schlenk technique. The 2-mercapto-4-methylpyrimidine hydrochloride (Hmpymt · HCl) and the sodium salt of ethanol were added to the solution of benzene, the mixture was stirred for 30 min, and then added organotin(IV) chlorides to the mixture, continuing the reaction about 12 h at 40 °C. After cooling down to room temperature, filtered it. The solvent of the filtrate was gradually removed by evaporation under vacuum until solid product was obtained. The details of synthetic experiments of complexes **1**–**11** were shown in Table 1.

2.2.1. $Ph_3Sn(SC_5H_5N_2)$ (**1**)

Recrystallized from ether–dichloromethane; m.p. 131–133 °C. Yield, 80%. Anal. Calc. for $C_{23}H_{20}N_2SSn$: C, 58.14; H, 4.24; N, 5.92. Found: C, 58.16; H, 4.21; N, 5.89. IR (KBr, cm^{-1}): 1632 (C=N), 701 (s, C–S), 560 (m, Sn–C), 448 (w, Sn ← N), 317 (m, Sn–S). ^{1}H NMR ($CDCl_3$): δ 7.36–7.79 ($^2J_{SnH}$ = 56 Hz, 15H), 1.33 (s, 3H), 6.71(d, 1H, J_{HH} = 6 Hz), 8.20 (d, 1H, J_{HH} = 9 Hz). ^{13}C NMR ($CDCl_3$): δ 172.87 (C2), 167.54 (C4), 156.51 (C6), 115.85 (C5), 23.35 (4-CH_3), 128.2 (*m*-C), 129.3 (*p*-C), 136.7 (*o*-C), 142.6 (*i*-C). ^{119}Sn NMR ($CDCl_3$, 298 K): −57 ppm.

2.2.2. $(PhCH_2)_3Sn(SC_5H_5N_2)$ (**2**)

Recrystallized from hexane–dichloromethane; m.p. 148–150 °C. Yield, 85%. Anal. Calc. for $C_{26}H_{26}N_2SSn$: C, 60.38; H, 5.67; N, 5.44. Found: C, 60.33; H, 5.64; N 5.41. IR (KBr, cm^{-1}): 1631(C=N), 702 (s, C–S), 562 (m, Sn–C), 450 (w, Sn ← N), 315 (m, Sn–S). ^{1}H NMR ($CDCl_3$): δ 7.46–7.79 (m, 15H), 3.26 ($^2J_{SnH}$ = 66 Hz, 6H, CH_2–Ph), 2.32 (s, 3H), 6.66 (d, 1H, J_{HH} = 6 Hz), 7.79 (d, 1H, J_{HH} = 9 Hz). ^{13}C NMR: δ 181.76 (C2), 172.54 (C4), 156.97 (C6), 117.85 (C5), 24.09 (CH_3), 37.5 (CH_2–Ph, $^1J_{SnC}$ = 330 Hz), 127.4 (*m*-C), 128.2 (*p*-C), 127.3(*o*-C), 124.2 (*i*-C). ^{119}Sn NMR ($CDCl_3$, 298 K): −55 ppm.

2.2.3. $(n\text{-}Bu)_3Sn(SC_5H_5N_2)$ (**3**)

Recrystallized from hexane–dichloromethane; m.p. 86–88 °C. Yield, 70%. Anal. Calc. for $C_{17}H_{32}N_2SSn$:

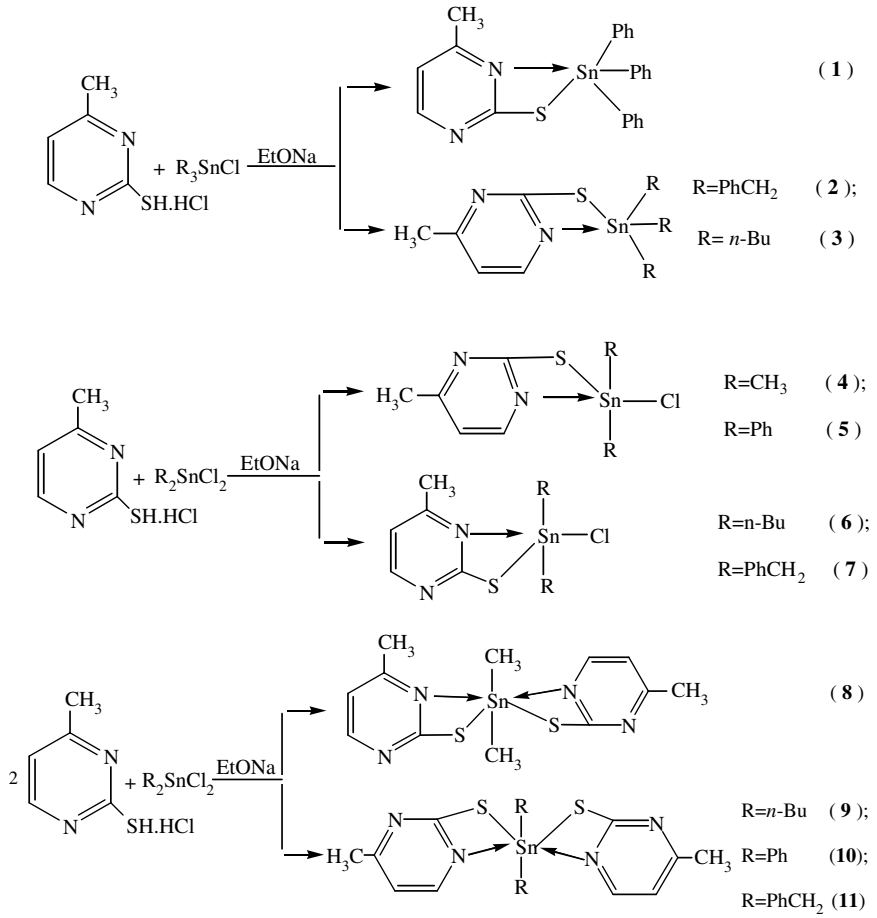

Scheme 1.

Table 1
The details of synthetic experiments of complexes **1**–**11**

Complexes	R_mSnCl_n	R_mSnCl_n:Hmpymt · HCl:EtONa	Products
1	Ph_3SnCl	1:1:2	$Ph_3Sn(SC_5H_5N_2)$
2	$(PhCH_2)_3SnCl$	1:1:2	$(PhCH_2)_3Sn(SC_5H_5N_2)$
3	$(n\text{-}Bu)_3SnCl$	1:1:2	$(n\text{-}Bu)_3Sn(SC_5H_5N_2)$
4	$(CH_3)_2SnCl_2$	1:1:2	$Me_2ClSn(SC_5H_5N_2)$
5	Ph_2SnCl_2	1:1:2	$Ph_2ClSn(SC_5H_5N_2)$
6	$(n\text{-}Bu)_2SnCl_2$	1:1:2	$(n\text{-}Bu)_2ClSn(SC_5H_5N_2)$
7	$(PhCH_2)_2SnCl_2$	1:1:2	$(PhCH_2)_2ClSn(SC_5H_5N_2)$
8	$(CH_3)_2SnCl_2$	1:2:4	$Me_2Sn(SC_5H_5N_2)_2$
9	$(n\text{-}Bu)_2SnCl_2$	1:2:4	$(n\text{-}Bu)_2Sn(SC_5H_5N_2)_2$
10	Ph_2SnCl_2	1:2:4	$Ph_2Sn(SC_5H_5N_2)_2$
11	$(PhCH_2)_2SnCl_2$	1:2:4	$(PhCH_2)_2Sn(SC_5H_5N_2)_2$

C, 48.21; H, 7.77; N, 6.75. Found: C, 48.19; H, 7.75; N 6.72. IR (KBr, cm^{-1}): 1631(C=N), 703 (s, C–S), 565 (m, Sn–C), 453 (w, Sn ← N), 318 (m, Sn–S). ^1H NMR ($CDCl_3$): δ 1.26–1.75 ($^2J_{SnH}$ = 69 Hz, 18H), 0.89 (t, 9H), 2.31 (s, 3H), 6.68 (d, 1H, J_{HH} = 7 Hz), 7.80 (d, 1H, J_{HH} = 10 Hz). ^{13}C NMR: δ 181.79 (C2), 172.56 (C4), 156.77 (C6), 118.85 (C5), 24.11 (CH_3), 13.6, 26.4, 27.6, 29.7 (^{n}Bu). ^{119}Sn NMR ($CDCl_3$, 298 K): −51 ppm.

2.2.4. *$Me_2ClSn(SC_5H_5N_2)$ (**4**)*

Recrystallized from hexane–dichloromethane; m.p. 124–126 °C. Yield, 78%. Anal. Calc. for $C_7H_{11}ClN_2SSn$: C, 27.18; H, 3.58; N, 9.09. Found: C, 27.15; H, 3.55; N 9.06. IR (KBr, cm^{-1}): 1631(C=N), 700 (s, C–S), 569 (m, Sn–C), 480 (w, Sn ← N), 318 (m, Sn–S), 272 (m, Sn–Cl). ^1H NMR ($CDCl_3$): δ 0.91 ($^2J_{SnH}$ = 72 Hz, 6H), 2.38 (s, 3H), 6.76 (d, 1H, J_{HH} = 7 Hz), 7.81 (d, 1H, J_{HH} = 12

Hz). ^{13}C NMR ($CDCl_3$): δ 181.83 (C2), 172.56 (C4), 156.97 (C6), 117.75 (C5), 24.06 (4-CH_3), 10.6 (CH_3, $^1J_{SnC}$ = 490 Hz). ^{119}Sn NMR ($CDCl_3$, 298 K): −77.6 ppm.

*2.2.5. $Ph_2ClSn(SC_5H_5N_2)$ (**5**)*

Recrystallized from hexane–dichloromethane; m.p. 120–122 °C. Yield, 76%. Anal. Calc. for $C_{17}H_{17}ClN_2SSn$: C, 47.12; H, 3.95; N, 6.46. Found: C, 47.10; H, 3.92; N 6.43. IR (KBr, cm^{-1}): 1631(C=N), 701 (s, C–S), 568 (m, Sn–C), 483 (w, Sn ← N), 318 (m, Sn–S), 280 (m, Sn–Cl). δ 7.45–7.91 ($^2J_{SnH}$ = 74 Hz, 10H), 2.33 (s, 3H), 6.69 (d, 1H, J_{HH} = 7 Hz), 8.22 (d, 1H, J_{HH} = 10 Hz). ^{13}C NMR ($CDCl_3$): δ 179.79 (C2), 170.56 (C4), 156.64 (C6), 116.97 (C5), 23.69 (4-CH_3), 124.7 ($^3J_{SnC}$ = 50 Hz, *m*-C), 129.6 ($^4J_{SnC}$ = 12 Hz, *p*-C), 136.9 ($^2J_{SnC}$ = 36 Hz, *o*-C), 146.5 ($^1J_{SnC}$ = 597 Hz, *i*-C). ^{119}Sn NMR ($CDCl_3$, 298 K): −175 ppm.

*2.2.6. $(n\text{-}Bu)_2ClSn(SC_5H_5N_2)$ (**6**)*

Recrystallized from hexane–dichloromethane; m.p. 100–102 °C. Yield, 75%. Anal. Calc. for $C_{13}H_{23}ClN_2SSn$: C, 39.67; H, 5.89; N, 7.12. Found: C, 39.65; H, 5.91; N 7.10. IR (KBr, cm^{-1}): 1631(C=N), 703 (s, C–S), 561 (m, Sn–C), 481(w, Sn ← N), 316 (m, Sn–S), 273 (m, Sn–Cl). ^{1}H NMR ($CDCl_3$): δ 1.57–1.75 ($^2J_{SnH}$ = 70 Hz, 12H), 0.87 (t, 6H), 1.37 (s, 3H), 6.68 (d, 1H, J_{HH} = 6 Hz), 8.23 (d, 1H, J_{HH} = 13 Hz). ^{13}C NMR ($CDCl_3$): δ 181.86 (C2), 172.66 (C4), 156.92 (C6), 117.55 (C5), 24.07 (4-CH_3), 24.11 (4-CH_3), 13.6, 26.4, 27.6, 29.7 (^{n}Bu, $^1J_{SnC}$ = 494 Hz, $^2J_{SnC}$ = 36.6 Hz, $^3J_{SnC}$ = 101.7 Hz). ^{119}Sn NMR ($CDCl_3$, 298 K): −76.2 ppm.

*2.2.7. $(PhCH_2)_2SnCl(SC_5H_5N_2)$ (**7**)*

Recrystallized from ether–dichloromethane; m.p. 146–148 °C. Yield, 72%. Anal. Calc. for $C_{19}H_{19}ClN_2SSn$: C, 49.44; H, 4.15; N, 6.10. Found: C, 49.41; H, 4.11; N, 6.07. IR (KBr, cm^{-1}): 1635(C=N), 701 (s, C–S), 561 (m, Sn–C), 475 (w, Sn ← N) 316 (m, Sn–S), 278 (m, Sn–Cl). ^{1}H NMR ($CDCl_3$): δ 7.46–7.79 (m, 15H), 3.29 ($^2J_{SnH}$ = 87 Hz, 4H), 1.35 (s, 3H), 6.69 (d, 1H, J_{HH} = 7 Hz), 8.22 (d, 1H, J_{HH} = 13 Hz). ^{13}C NMR ($CDCl_3$): δ 179.76 (C2), 170.52 (C4), 156.67 (C6), 116.93 (C5), 23.69 (4-CH_3), 38.5 (CH_2–Ph, $^1J_{SnC}$ = 650 Hz), 125.4 ($^4J_{SnC}$ = 30 Hz, *m*-C), 127.0 ($^5J_{SnC}$ = 26 Hz, *p*-C), 130.5 ($^3J_{SnC}$ = 44 Hz, *o*-C), 139.0 ($^2J_{SnC}$ = 36 Hz, *i*-C). ^{119}Sn NMR ($CDCl_3$, 298 K): −172 ppm.

*2.2.8. $Me_2Sn(SC_5H_5N_2)_2$ (**8**)*

Recrystallized from ether; m.p. 218–210 °C. Yield, 85%. Anal. Calc. for $C_{12}H_{16}N_4S_2Sn$: C, 36.11; H, 4.04; N, 14.10. Found: C, 36.08; H, 4.01; N, 14.06. IR (KBr, cm^{-1}): 1635 (m, C=N), 700 (s, C–S), 567 (m, Sn–C), 488 (w, Sn ← N), 320 (m, Sn–S). ^{1}H NMR ($CDCl_3$): δ 1.05 (s, 6H, $^2J_{SnH}$ = 80 Hz), 1.31 (s, 3H), 2.36 (s, 3H), 6.68 (d, 1H, J_{HH} = 7 Hz), 6.75 (d, 1H, J_{HH} = 8 Hz), 7.83 (d, 1H, J_{HH} = 10 Hz), 8.24 (d, 1H, J_{HH} = 12 Hz). ^{13}C NMR ($CDCl_3$): δ 181.79, 179.73 (C2), 171.72, 166.7 (C4), 157.41, 156.45 (C6), 117.78, 115.2 (C5), 24.01, 23.84 (4-CH_3), 10.9 (CH_3, $^1J_{SnC}$ = 546 Hz). ^{119}Sn NMR ($CDCl_3$, 298 K): −121 ppm.

*2.2.9. $(n\text{-}Bu)_2Sn(SC_5H_5N_2)_2$ (**9**)*

Recrystallized from ether–dichloromethane; m.p. 220 °C (dec.). Yield, 74%. Anal. Calc. for $C_{18}H_{28}N_4S_2Sn$: C, 44.74; H, 5.84; N, 11.64. Found: C, 44.72; H, 5.81; N, 11.60. IR (KBr, cm^{-1}): 1635 (m, C=N), 701 (s, C–S), 563 (m, Sn–C), 453 (w, Sn ← N), 319 (m, Sn–S). ^{1}H NMR ($CDCl_3$): δ 1.10–1.75 ($^2J_{SnH}$ = 73 Hz, –$CH_2CH_2CH_2$); 0.95 (t, –CH_3), 2.31 (s, 6H), 6.69 (d, 2H, J_{HH} = 8 Hz), 7.83 (d, 2H, J_{HH} = 13 Hz). ^{13}C NMR ($CDCl_3$): δ 181.79 (C2), 171.72 (C4), 157.81 (C6), 117.41 (C5), 23.96 (4-CH_3), 13.6, 26.4, 27.6, 29.7 (^{n}Bu, $^1J_{SnC}$ = 515 Hz, $^2J_{SnC}$ = 38 Hz, $^3J_{SnC}$ = 106 Hz). ^{119}Sn NMR ($CDCl_3$, 298 K): −81 ppm.

*2.2.10. $Ph_2Sn(SC_5H_5N_2)_2$ (**10**)*

Recrystallized from ether–dichloromethane; m.p. 193–195 °C. Yield, 76%. Anal. Calc. for $C_{22}H_{20}N_4S_2Sn$: C, 50.50; H, 3.85; N, 10.75. Found: C, 50.47; H, 3.81; N, 10.71. IR (KBr, cm^{-1}): 1635 (m, C=N), 701 (s, C–S), 564 (m, Sn–C), 460 (w, Sn ← N), 320 (m, Sn–S). ^{1}H NMR ($CDCl_3$): δ 7.45–7.91 ($^2J_{SnH}$ = 75 Hz, 15H), 2.32 (s, 6H), 6.68 (d, 2H, J_{HH} = 7 Hz), 8.01 (d, 2H, J_{HH} = 12 Hz). ^{13}C NMR ($CDCl_3$): δ 181.78 (C2), 171.69 (C4), 155.74 (C6), 117.53(C5), 24.02 (4-CH_3), 128.6 ($^3J_{SnC}$ = 53 Hz, *m*-C), 129.3 ($^4J_{SnC}$ = 18 Hz, *p*-C), 134.5 ($^2J_{SnC}$ = 33 Hz, *o*-C), 146.5 ($^1J_{SnC}$ = 561 Hz, *i*-C). ^{119}Sn NMR ($CDCl_3$, 298 K): −129 ppm.

*2.2.11. $(PhCH_2)_2Sn(SC_5H_5N_2)_2$ (**11**)*

Recrystallized from ether–dichloromethane; m.p. 128–130 °C. Yield, 82%. Anal. Calc. for $C_{24}H_{24}N_4S_2Sn$: C, 52.29; H, 4.39; N, 10.21. Found: C, 52.25; H, 4.36; N, 10.21. IR (KBr, cm^{-1}): 1635 (m, C=N), 701 (s, C–S), 561 (m, Sn–C), 473 (w, Sn ← N), 321 (m, Sn–S). ^{1}H NMR ($CDCl_3$): δ 7.46–7.79 (m, 15H), 3.47 ($^2J_{SnH}$ = 83 Hz, 6H, CH_2–Ph), 2.35 (s, 6H, J_{HH} = 6 Hz), 6.67 (d, 2H, J_{HH} = 12 Hz), 7.82 (d, 2H). ^{13}C NMR ($CDCl_3$): δ 181.73 (C2), 171.78 (C4), 157.89 (C6), 117.64(C5), 24.07 (4-CH_3), 37.3 (CH_2–Ph, $^1J_{SnC}$ = 686 Hz), 127.4 ($^4J_{SnC}$ = 31 Hz, *m*-C), 128.2 ($^5J_{SnC}$ = 25 Hz, *p*-C), 127.3 ($^3J_{SnC}$ = 48 Hz, *o*-C), 124.2 ($^2J_{SnC}$ = 34 Hz, *i*-C). ^{119}Sn NMR ($CDCl_3$, 298 K): −257 ppm.

*2.3. X-ray structure analyses of **1**, **2**, **4**, **5**, **7**, **8**–**11***

Crystals were mounted in Lindemann capillaries under nitrogen. Diffraction data were collected on a

Smart–1000 CCD area-detector with graphite monochromated Mo Kα radiation ($\lambda = 0.71073$ Å). A semi-empirical absorption correction was applied to the data. The structure was solved by direct methods using SHELXS-97 and refined against F^2 by full matrix least-squares using SHELXL-97. Hydrogen atoms were placed in calculated positions. Crystal data and experimental details of the structure determinations of **1** and **2**, **4**, **5** and **7**, and **8**–**11** are listed in Tables 2–4, respectively.

3. Results and discussion

3.1. Spectra

The IR spectra show that the strong absorption at 2650 cm^{-1} in free ligand due to the –SH group is absent in spectra of all complexes **1**–**11**, while new absorption appears in 315–321 cm^{-1} region. All these values are located within the range for Sn–S vibration observed in common organotin derivatives of thiolate (300–400 cm^{-1}) [15], consequently, they can be assigned to ν(Sn–S). The middle intensity bands observed at 1635 cm^{-1} in the spectra of all complexes **1**–**11** have been assignable to ν(C=N) according to literatures [16,17] Furthermore, the weak- or medium-intensity absorptions at the region of 448–483 cm^{-1} in all complexes **1**–**11** have been assigned to Sn ← N vibration [18]. The ν(Sn–Cl) absorptions at the region of 272–280 cm^{-1} in complexes **4**–**7** are close to those found in trichloromethylbis(imidazole)tin · H_2O (275 cm^{-1}) and $(PhCH_2)_2SnCl$ (BzACDA) (282 cm^{-1}) [19,20].

In the ^{1}H NMR spectrum, one methyl signal has similar chemical shift at the region of 1.33–1.35 ppm in complexes **1**, **6** and **7**, similar methyl groups signal appears at the region of 2.31–2.38 ppm in complexes **2**, **3**, **4**, **5** and **9**–**11**, while two methyl signals appear at both 2.36 and 1.31 ppm in complex **8**. These results mean that adjacent isomer **A** of mpymt ligand exists in complexes **1**, **6** and **7**, remote isomer **B** exists in complexes **2**, **3**, **4**, **5** and **9**–**11**, while both remote and adjacent coordination modes exist in complex **8**, respectively.

The ^{13}C NMR spectra of all complexes **1**–**11** show a significant downfield shift of all carbon resonances. The shift is a consequence of an electron density transfer from the ligand to the acceptor. The $^nJ(^{119}Sn–^{13}C)$ coupling constants were detected in the case of sufficiently soluble derivatives. In complexes **4**–**7**, the order of magnitude of the coupling constants is the same as those previously reported for analogous five-coordinate derivatives [7], whereas in the case of derivatives **8**–**11**, the $^nJ(^{119}Sn–^{13}C)$

Table 2
Crystal, data collection and structure refinement parameters of complexes **1** and **2**

Complexes	**1**	**2**
Empirical formula	$C_{23}H_{20}N_2SSn$	$C_{26}H_{26}N_2SSn$
Formula weight	475.16	517.24
Wavelength (Å)	0.71073	0.71073
Crystal system	Orthorhombic	Triclinic
Space group	*Pbca*	$\bar{P}$
a (Å)	9.450(5)	12.262(16)
b (Å)	15.544(8)	14.122(18)
c (Å)	28.197(13)	14.369(19)
α (°)	90	78.42(2)
β (°)	90	80.331(19)
γ (°)	90	89.329(19)
V (Å^3)	4142(3)	2402(5)
Z	4	4
D_{calc} (Mg m^{-3})	1.524	1.430
F(000)	1904	1048
μ (mm^{-1})	1.344	1.165
Crystal size (mm)	0.450.38 × 0.32	0.45 × 0.37 × 0.13
θ Range	1.44–25.03	1.47–25.03
Index ranges	$-11 \leqslant h \leqslant 11$; $-18 \leqslant k \leqslant 16$; $-30 \leqslant l \leqslant 33$	$-14 \leqslant h \leqslant 13$; $-16 \leqslant k \leqslant 16$; $-17 \leqslant l \leqslant 11$
Reflections collected	20384	12351
Unique reflections	3655(R_{int} = 0.0460)	8401(R_{int} = 0.0257)
Absorbtion correction	Semi-empirical from equivalents	Semi-empirica from equivalents
Max/min transmission	0.6730, 0.5830	0.8633, 0.6222
Data, restrainst, parameters	3655, 0, 244	8401, 0, 541
GOF	1.133	0.866
Final R indices [$I > 2\sigma(I)$]	R_1 = 0.0352, wR_2 = 0.0830	R_1 = 0.0389 wR_2 = 0.0711
R indices (all data)	R_1 = 0.0583, wR_2 = 0.1029	R_1 = 0.0768, wR_2 = 0.0806
Largest difference peak, hole (e Å^{-3})	0.538, −0.405	0.603, −0.481

Table 3
Crystal, data collection and structure refinement parameters of complexes **4**, **5** and **7**

Complexes	**4**	**5**	**7**
Empirical formula	$C_7H_{11}N_2SClSn$	$C_{17}H_{15}ClN_2SSn$	$C_{19}H_{19}N_2SClSn$
Formula weight	309.38	433.51	461.56
Wavelength (Å)	0.71073	0.71073	0.71073
Crystal system	Monoclinic	Orthorhombic	Orthorhombic
Space group	*C*2/*m*	*Pca*2$_1$	*Pnma*
a (Å)	20.456(10)	21.899(10)	11.495(11)
b (Å)	7.613(4)	9.544(4)	15.353(15)
c (Å)	7.549(4)	17.274(8)	10.846(11)
α (°)	90	90	90
β (°)	95.056(8)	90	90
γ (°)	90	90	90
V (Å^3)	1171.1(10)	3610(3)	1914(3)
Z	4	8	4
D_{calc} (Mg m^{-3})	1.755	1.595	1.602
F(000)	600	1712	920
μ (mm^{-1})	2.544	1.676	1.586
Crystal size (mm)	0.50 × 0.40 × 0.29	0.53 × 0.44 × 0.13	0.45 × 0.29 × 0.25
θ Range	2.00–25.02	1.86–25.02	2.30–25.02
Index ranges	$-21 \leqslant h \leqslant 24$	$-25 \leqslant h \leqslant 26$	$-12 \leqslant h \leqslant 13$
	$-9 \leqslant k \leqslant 8$	$-11 \leqslant k \leqslant 11$	$-18 \leqslant k \leqslant 16$
	$-8 \leqslant l \leqslant 8$	$-15 \leqslant l \leqslant 20$	$-12 \leqslant l \leqslant 12$
Reflections collected	3087	18 140	9529
Unique reflections	1109(R_{int} = 0.0888)	5464(R_{int} = 0.0438)	1761(R_{int} = 0.0362)
Absorbtion correction	Semi-empirical from equivalents	Semi-empirical from equivalents	Semi-empirical from equivalents
Max/min transmission	0.5258, 0.3628	0.8116, 0.4703	0.6925, 0.5355
Data, restrainst, parameters	1109, 0, 70	5464, 1, 397	1761, 0, 124
GOF	1.021	0.935	1.113
Final *R* indices [$I > 2\sigma(I)$]	R_1 = 0.0504 wR_2 = 0.1134	R_1 = 0.0312 wR_2 = 0.0606	R_1 = 0.0298, wR_2 = 0.0682
R indices (all data)	R_1 = 0.0767, wR_2 = 0.1522	R_1 = 0.0494 wR_2 = 0.0657	R_1 = 0.0426, wR_2 = 0.0754
Largest difference peak, hole (e Å^{-3})	0.959, −0.548	0.273, −0.297	0.569, −0.390

are close to those found for six-coordinate skewed trapezoidal diorganotin(IV) complexes [21,22].

For methyl derivatives **4** and **8**, substitution of $^2J(^{119}Sn–^1H)$ values (72 and 80 Hz, respectively) and $^1J(^{119}Sn–^{13}C)$ values (490 and 546 Hz, respectively) into the corresponding Lockhart–Marders equations [22–24] (empirical relationship between the coupling constants and the C–Sn–C angle) gives C–Sn–C angle values of 121° and 119° for complex **4** and 130° and 124° for complex **8**, respectively. These angles values might suggest that in solution the dimethyltin derivative **4** is a distorted trigonal bipyramid, while complex **8** is a skew-trapezoidal bipyramid and the basic features of the solid-state phase remain in $CDCl_3$ solution.

As reported in literatures [25], values of δ (^{119}Sn) in the ranges −210 to −400, −90 to −190 and 200 to −60 ppm have been associated with six-, five- and four-coordinate tin centers, respectively. On this base, the ^{119}Sn NMR spectra of triorganotin (IV) derivatives **1**–**3** show one broad sharp signal and show rather temperature-dependent. The δ values found (−57, −55 and −51 ppm at 298 K and lower values at 195 K, −87, −85 and −80 ppm, respectively) are consistent with a tetrahedral and monomeric structure caused by the weaker Sn–N bonds. Besides, the ^{119}Sn NMR chemical shifts of **4**–**7** are in accordance with those of five coordinate diorganotin(IV) halides complexes involving halide or phosphine lignds [26], as well as chelating S-donors and O-donors complexes [27,28]. Five-coordinate $ClPh_2SnXY$ compounds (X and Y = electronegative groups) in solution have ^{119}Sn NMR values in the region −140 to −180 ppm depending on the groups present [29,30] and are rather independent of the temperature. For example, the spectrum of complex **5** reveals one narrow signal in the whole temperature range. The value of ^{119}Sn chemical shift changes only slightly with a decrease in the temperature (−175 ppm at 298 K and −180 ppm at 195 K, respectively). Which suggests that the Sn–N interaction probably survives in solution and that a five-coordinate species is maintained. While the ^{119}Sn NMR chemical shift of **8**–**11** are not informative enough. The chemical shift values of complexes **8** and **11** are −121, −257 ppm at 298 K, and −125, −260 ppm at 195 K, respectively. Which can belong to penta- or weakly hexacoordinated diorganotin(IV) complexes [31,32]. While the values of complexes **9** and **10** are −81, −129 ppm at 298 K, and −123, −229 ppm at 195 K, respectively, which indicated that complexes **9** and **10** are rather temperature-dependent than the complexes **8** and **11**, and the

Table 4
Crystal, data collection and structure refinement parameters of complexes **8**–**11**

Complexes	**8**	**9**	**10**	**11**
Empirical formula	$C_{12}H_{16}N_4S_2Sn$	$C_{18}H_{28}N_4S_2Sn$	$C_{22}H_{20}N_4S_2Sn$	$C_{24}H_{24}N_4S_2Sn$
Formula weight	399.10	483.25	523.23	551.28
Wavelength (Å)	0.71073	0.71073	0.71073	0.71073
Crystal system	Orthorhombic	Monoclinic	Monoclinic	Orthorhombic
Space group	$Cmc2_1$	$P2_1/n$	$P2_1/n$	$Pna2_1$
a (Å)	7.582(4)	6.178(7)	9.933(3)	11.350(12)
b (Å)	17.751(8)	43.14(5)	16.626(6)	11.550(12)
c (Å)	12.063(6)	8.774(10)	14.388(5)	18.629(20)
α (°)	90	99.324(16)	108.390(5)	90
V (Å^3)	1623.5(13)	2307(4)	2255.0(13)	2442(4)
Z	4	4	4	4
D_{calc} (g m^{-3})	1.633	1.391	1.541	1.499
$F(000)$	792	984	1048	1112
μ (mm^{-1})	1.823	1.296	1.334	1.236
Crystal size (mm)	$0.42 \times 0.23 \times 0.20$	$0.46 \times 0.110.09$	$0.32 \times 0.25 \times 0.17$	$0.41 \times 0.34 \times 0.02$
θ Range	2.29–25.02	1.89–25.03	1.93–25.02	2.07–25.03
Index ranges	$-9 \leqslant h \leqslant 8$; $-17 \leqslant k \leqslant 121$; $-14 \leqslant l \leqslant 14$	$-7 \leqslant h \leqslant 7$; $-32 \leqslant k \leqslant 51$; $-10 \leqslant l \leqslant 10$	$-11 \leqslant h \leqslant 11$; $-12 \leqslant k \leqslant 19$; $-17 \leqslant l \leqslant 16$	$-13 \leqslant h \leqslant 13$; $-13 \leqslant k \leqslant 12$; $-22 \leqslant l \leqslant 14$
Reflections collected	4230	11 228	11 753	12207
Unique reflections	1515(R_{int} = 0.0292)	3835(R_{int} = 0.051)	3981(R_{int} = 0.0622)	3340(R_{int} = 0.0297)
Absorbtion correction	Semi-empirical from equivalents	Semi-empirical from equivalents	Semi-empirical from equivalents	Semi-empirical from equivalents
Max/min transmission	0.7119, 0.5147	0.8923, 0.5670	0.8050, 0.6749	0.9793, 0.6313
Data, restrainst, parameters	1515, 1, 112	3835,10, 226	3981, 0, 262	3340, 1, 280
GOF	0.907	1.028	0.829	1.014
Final R indices [$I > 2\sigma(I)$]	R_1 = 0.0264, wR_2 = 0.0527	R_1 = 0.0667 wR_2 = 0.1383	R_1 = 0.0394 wR_2 = 0.0639	R_1 = 0.0263, wR_2 = 0.0629
R indices (all data)	R_1 = 0.0331, wR_2 = 0.0542	R_1 = 0.1096, wR_2 = 0.1552	R_1 = 0.0810, wR_2 = 0.0728	R_1 = 0.0335, wR_2 = 0.0670
Largest difference peak, hole (e Å^{-3})	0.526, −0.180	0.623, −0.856	0.820, −0.426	0.561, −0.260

Sn–N bonds are probably dissociated with increase of the temperature.

From our NMR data for all complexes and following structural studied, we conclude that the nitrogen ligand is labile and hence that the mechanism of interaction of organotin complexes in biological systems differs from that of platinum complexes which retain the Pt–N bonds when reacting with DNA. In organotin compounds the Sn–N bonds are probably cleaved before the tin reaches its ultimate target.

3.2. Description of crystal structures

3.2.1. $Ph_3Sn(SC_5H_5N_2)$ (**1**) and $(PhCH_2)_3Sn(SC_5H_5N_2)$ (**2**)

Selected bond lengths and bond angles for **1** and **2** are given in Table 5 and their molecular structures and the packing of cell units of complexes **1** and **2** are shown in Fig. 2–5, respectively.

The four primary bonds to Sn in **1** are to three phenyl groups [Sn–C between 2.135(4) and 2.152(5) Å] and to S [Sn(1)–S(1) distance 2.4228(16) Å], in addition there is a weak intramolecular Sn–N interaction [Sn(1)–N(2) distance 2.907(4) Å], thus providing a 4-membered chelate ring. The Sn–S bond length in **1** lies in the middle of the range reported for triphenyltin heteroarenethiolates (2.405–2.481 Å) and approach the sum of the covalent radii of tin and sulfur (2.42 Å) [33,34], which prove that sulfur atoms coordinated to tin atom by strong covalent bonds. Besides, the Sn–N distance is little longer than that of complex $Ph_3Sn(Me_2Pymt)$ (2.835(7) Å) [11], but still shorter than the sum of the van der Waals radii of tin and nitrogen (3.74 Å) [35]. So it can be regarded as a weak coordination bond. In contrast, for complex **2**, the Sn(1)–S(1) bond length and the Sn(1)–N(1) distance are 2.455(2) and 2.885(5) Å, all of them are similar to those of complex **1**.

Including the tin–nitrogen interaction [36], the geometry at Sn in complexes **1** and **2** becomes distorted trigonal bipyramidal with the axial–tin–axial angles N(2)–Sn(1)–C(12) of 155.50(14)° for complex **1** and N(1)–Sn(1)–C(20) of 158.45(15)° for complex **2**, respectively.

It is worth to note that in tri–organotin complexes, the coordination mode **B** is preferred to be selected than the mode **A** because of the stereo-constraints of tri-alkyl and this is the case of the complex **2**, as shown in Fig. 4. However, to our surprise, we find that the ligand choose the coordination mode **A** in complex **1** irrespective of the steric hindrance, as shown in Fig. 2, which maybe attribute to the ring-stacking interactions. The orientation is

Table 5
Selected bond lengths and angles for the complexes **1** and **2**

Complex 1		Complex 2	
Bond	Distance (Å)	Bond	Distance (Å)
Sn(1)–C(18)	2.135(4)	Sn(1)–C(13)	2.151(5)
Sn(1)–C(6)	2.136(5)	Sn(1)–C(6)	2.152(5)
Sn(1)–C(12)	2.152(5)	Sn(1)–C(20)	2.174(5)
Sn(1)–S(1)	2.4228(16)	Sn(1)–S(1)	2.455(2)
Sn(1)–N(2)	2.907(4)	Sn(1)–N(1)	2.885(5)
S(1)–C(1)	1.755(5)	S(1)–C(1)	1.763(5)
Angle	Amplitude (°)	Angle	Amplitude (°)
C(18)–Sn(1)–C(6)	110.19(17)	C(13)–Sn(1)–C(6)	116.86(19)
C(18)–Sn(1)–C(12)	107.65(16)	C(13)–Sn(1)–C(20)	107.34(19)
C(6)–Sn(1)–C(12)	109.74(16)	C(6)–Sn(1)–C(20)	108.8(2)
C(18)–Sn(1)–S(1)	117.06(12)	C(13)–Sn(1)–S(1)	113.93(15)
C(6)–Sn(1)–S(1)	113.79(12)	C(6)–Sn(1)–S(1)	108.77(14)
C(12)–Sn(1)–S(1)	97.34(12)	C(20)–Sn(1)–S (1)	99.62(15)
C(18)–Sn(1)–N(2)	85.42(14)	C(13) –Sn(1)–N(1)	81.73(15)
C(6)–Sn(1)–N(2)	83.67(14)	C(6)–Sn(1)–N(1)	82.87(18)
C(12)–Sn(1)–N(2)	155.50(14)	C(20)–Sn(1)–N(1)	158.45(15)
S(1)–Sn(1)–N(2)	58.17(8)	S(1)–Sn(1)–N(1)	58.98(10)

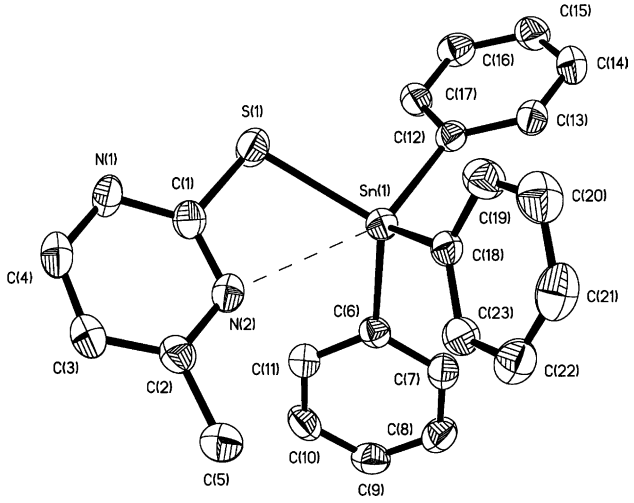

Fig. 2. Molecular structure of complex **1**.

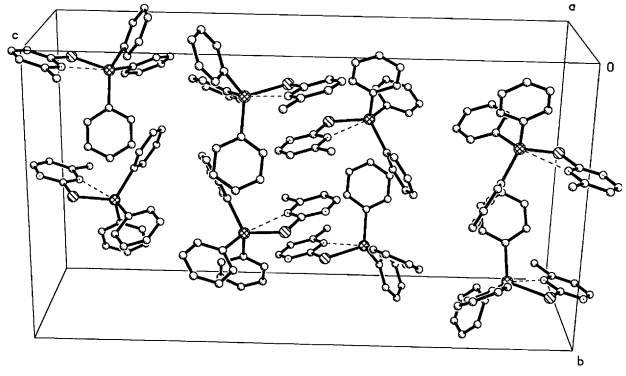

Fig. 3. The unit cell of complex **1**.

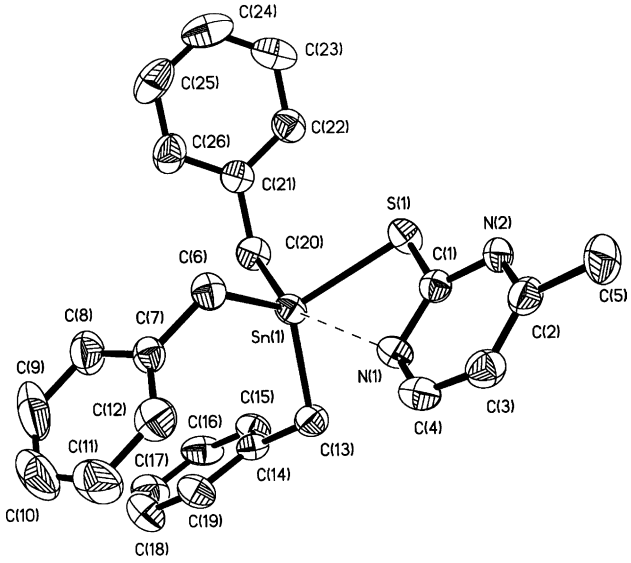

Fig. 4. Molecular structure of complex **2**.

such that each mpymt group is arranged face-to-face at a distance of 3.369 Å and shows significant π–π stacking interactions [37,38]. Furthermore, CH–π interactions between the Ph ring and the C-4 methyl group of the ligand also stabilize the structure, the distances C(5)···C(16), C(5)···C(17) and C(5)···C(12) are 3.776, 3.788 and 4.705 Å, respectively [39].

3.2.2. $Me_2SnCl(SC_5H_5N_2)$ (**4**), $Ph_2SnCl(SC_5H_5N_2)$ (**5**) and $(PhCH_2)_2SnCl(SC_5H_5N_2)$ (**7**)

Selected bond lengths and bond angles for **4**, **5** and **7** are given in Table 6–8, respectively. The molecular structures and unit cells of **4**, **5** and **7** are shown in Fig. 6–11, respectively.

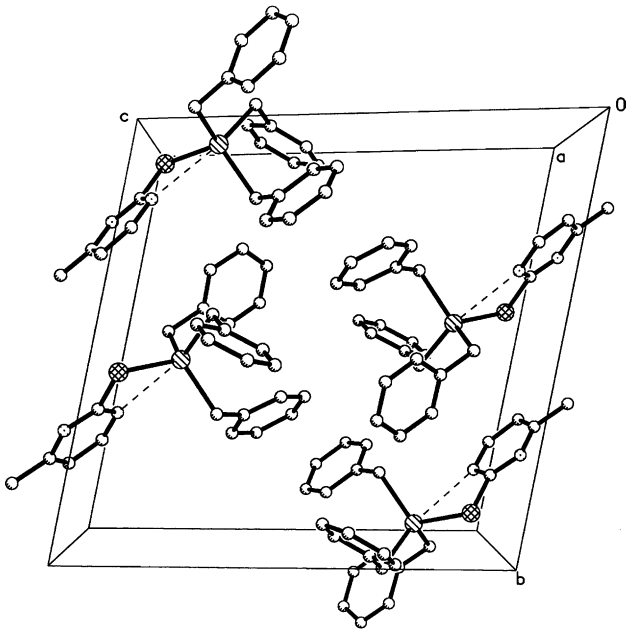

Fig. 5. The unit cell of complex **2**.

Different from those triorganotin chlorides, diorganotin dichlorides have two chlorine atoms that can be substituted. When diorganotin dichlorides react with Hmpymt in 1:1 molar ratio, one chlorine atom still remained, as shown in Figs. 6, 8 and 10, respectively. However, due to inter and/or intra-molecular interactions and steric requriements, the coordination mode of the ligand is different between complexes **4**, **5** and complex **7**.

For complex **4**, the coordination geometry about Sn(IV) is a distorted trigonal bipyramid in which two carbon atoms of two methyl groups and a sulfur atom form the equatorial plane, the sum of the trigonal plane angles is 354.4°, while one nitrogen atom and one halogen atom occupy the axial site [Cl(1)–Sn(1)–N(1) 153.9(3)°]. In this way the ligand behaves as a bidentate species and chelates the tin atom by means of the nirogen and the thiolato sulfur. The consequence formation of a four member ring with a S(1)–Sn(1)–N(1) bite angle 63.5(3)°. The Sn(1)–Cl(1) distance (2.454(4) Å) lies in the range of the covalent radii (2.37–2.60 Å) [40]. The

Table 6
Selected bond lengths and angles for the complex **4**

Bond	Distance (Å)	Bond	Distance (Å)
Sn(1)–C(6)	2.122(10)	Sn(1)–S(1)	2.459(4)
Sn(1)–C(6)#1	2.122(10)	Sn(1)–N (1)	2.509(11)
Sn(1)–Cl(1)	2.454(4)	Sn(1)···Cl(1A)	3.959
S(1)–C(1)	1.758(12)		
Angle	Amplitude (°)	Angle	Amplitude (°)
C(6)–Sn(1)–C(6)#1	123.4(6)	Cl(1)–Sn(1)–S(1)	90.44(13)
C(6)–Sn(1)–Cl(1)	101.4(3)	C(6)–Sn(1)–N(1)	90.7(3)
C(6)#1–Sn(1)–Cl(1)	101.4(3)	C(6)#1–Sn(1)–N(1)	90.7(3)
C(6)–Sn(1)–S (1)	115.5(3)	Cl(1)–Sn(1)–N(1)	153.9(3)
C(6)#1–Sn(1)–S (1)	115.5(3)	S(1)–Sn(1)–N(1)	63.5(3)
Sn(1)–Cl(1)···Sn(1A)	101.8		

Table 7
Selected bond lengths and angles for the complexes **5**

Molecule A		Molecule B	
Bond	Distance (Å)	Bond	Distance (Å)
Sn(1)–C(12)	2.116(8)	Sn(2)–C(29)	2.113(7)
Sn(1)–S(1)	2.418(2)	Sn(2)–S(2)	2.423(2)
Sn(1)–N(1)	2.483(5)	Sn(2)–N(3)	2.456(5)
Sn(1)–C(6)	2.141(6)	Sn(2)–C(23)	2.108(5)
Sn(1)–Cl(1)	2.4215(18)	Sn(2)–Cl(2)	2.4307(17)
S(1)–C (1)	1.743(6)	S(2)–C(18)	1.746(6)
Angle	Amplitude (°)	Angle	Amplitude (°)
C(12)–Sn(1)–C(6)	114.5(2)	C(23)–Sn(2)–C(29)	126.6(3)
C(12)–Sn(1)–S(1)	122.7(2)	C(23)–Sn(2)–S(2)	116.07(18)
C(6)–Sn(1)–S(1)	118.30(17)	C(29)–Sn(2)–S(2)	113.93(19)
C(12)–Sn(1)–Cl(1)	99.91(17)	C(23)–Sn(2)–Cl(2)	97.91(16)
C(6)–Sn(1)–Cl(1)	99.43(15)	C(29)–Sn(2)–Cl(2)	97.68(17)
C(12)–Sn(1)–N(1)	95.0(3)	C(23)–Sn(2)–N(3)	93.1(2)
S(1)–Sn(1)–N(1)	64.08(13)	S(1)–Sn(2)–N(1)	64.27(15)
S(1)–Sn(1)–Cl(1)	92.11(7)	S(2)–Sn(2)–Cl(2)	92.18(7)
C(6)–Sn(1)–N(1)	91.1(2)	C(29)–Sn(2)–N(3)	92.2(3)
Cl(1)–Sn(1)–N(1)	156.13(15)	Cl(1)–Sn(1)–N(1)	156.45(17)

Table 8
Selected bond lengths and angles for the complex **7**

Bond	Distance (Å)	Bond	Distance (Å)
Sn(1)–C(6)	2.144(4)	Sn(1)–N(1)	2.664(5)
Sn(1)–C(6)#1	2.144(4)	S(1)–C(1)	1.731(5)
Sn(1)–Cl(1)	2.424(3)	Sn···N	2.804
Sn(1)–S(1)	2.480(3)	Sn···S	3.672
Angle	Amplitude (°)	Angle	Amplitude (°)
C(6)–Sn(1)–C(6)#1	143.1(2)	C(6)–Sn(1)–N(1)	88.27(12)
C(6)–Sn(1)–Cl(1)	100.83(12)	C(6)#1–Sn(1)–N(1)	88.27(12)
C(6)#1–Sn(1)–Cl(1)	100.83(12)	Cl(1)–Sn(1)–N(1)	149.05(11)
C(6)–Sn(1)–S(1)	105.06(11)	S(1)–Sn(1)–N(1)	60.61(9)
C(6)#1–Sn(1)–S(1)	105.06(11)	S(1A)···Sn(1)···N(3A)	45.89
Cl(1)–Sn(1)–S(1)	88.44(6)		

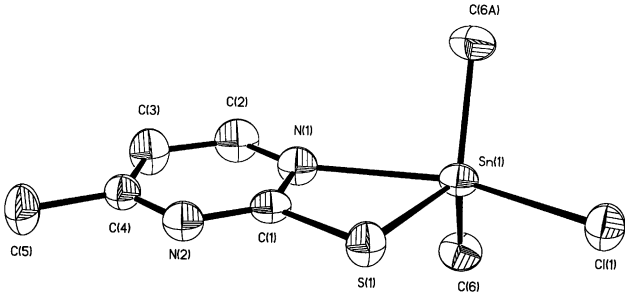

Fig. 6. Molecular structure of complex **4**.

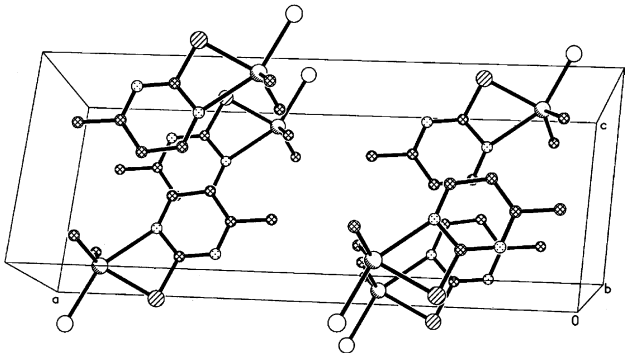

Fig. 7. The unit cell of complex **4**.

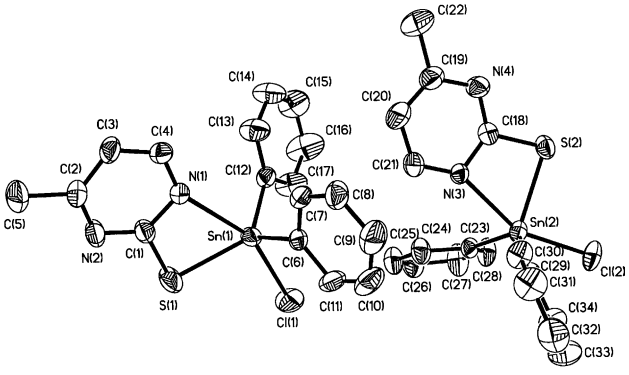

a **b**

Fig. 8. Molecular structure of complex **5**.

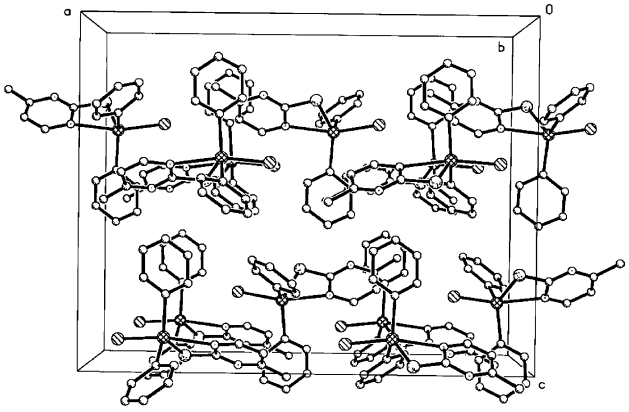

Fig. 9. The unit cell of complex **5**.

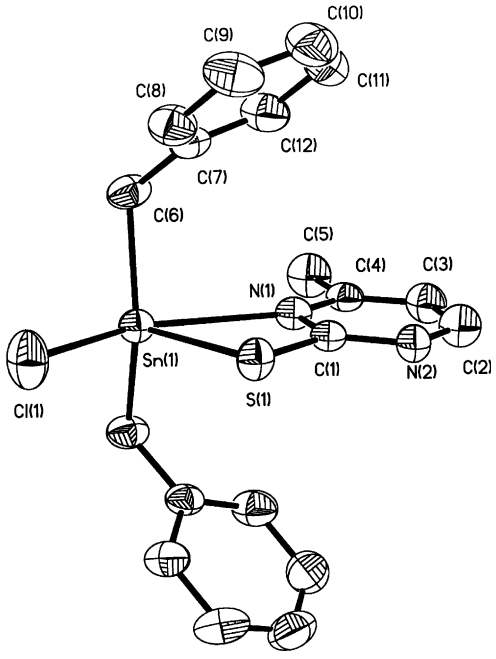

Fig. 10. Molecular structure of complex **7**.

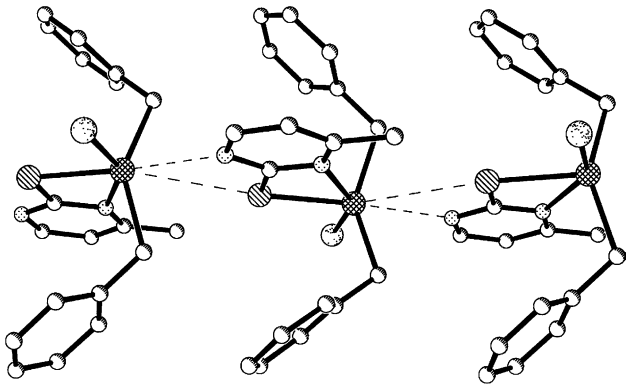

Fig. 11. Perspective view showing the 1D ribbon of the complex **7**.

Sn(1)–S(1) distance 2.459(4) Å, approach the covalent radii of Sn and S (2.42 Å) [34]. The Sn(1)–N(1) distance 2.509(11) Å, is consistent with that of [2-(Me_2NCH_2)C_6H_4]$SnPh_2Cl$ [2.519(2) Å] [40].

For complex **5**, as shown in Fig. 8, which contains two crystallographically independent molecules **a** and **b**. And the conformations of the two molecules are almost the same, only with little differences in bond lengths and bond angles (see Table 7). Both of the coordination geometries about Sn(IV) atoms are distorted trigonal bipyramid, similar to that of complex **4**. In which two phenyl groups and a sulfur atom form the equatorial plane, while the halogen and the nitrogen occupy the apical positions. The Sn–Cl distances are 2.4215(18) and 2.4307(17) Å, lies in the range (2.32–2.58 Å) of Sn–Cl distances found in chloroorganotin (IV) complexes in general [41,42]. The Sn–S distances are 2.418(2) and 2.423(2) Å, shorter than those of Ph_2SnCl(MBT) (2.485(22) Å) [43]. The Sn–N bond lengths are 2.483(5) and 2.456(5) Å, the bite angles N(1)–Sn(1)–S(1) 64.08(13)° and N(3)–Sn(2)–S(2) 64.27(15)°. All above of which are similar to those of complex **4**.

As far as complex **7** is concerned, the environment of tin is similar to that of complex **5** except for the coordination mode of mpymt ligand, in which the ligand adopts mode **A** to bond to tin atom. The geometry of Sn is also a distorted *cis*-trigonal bipyramidal with one nitrogen atom and one halogen atom in axial sites [Cl(1)–Sn(1)–N(1) 149.05(11)°], and one sulfur and two benzenyl C atoms occupying the equatorial plane [C(6)#1–Sn(1)–C(6) 143.1(2)°, C(6)–Sn(1)–S(1) 105.06(11)°, C(6)#1–Sn(1)–S(1) 105.06(11)°]. The Sn(1)–Cl(1) distance 2.424(3) Å, Sn(1)–N(2) distance 2.664(5) Å, and the Sn(1)–S(1) distance 2.480(3) Å, the bite angle N(1)–Sn(1)–S(1) 60.61(9)°, are all consistent with those of complex **5**.

It is worth to note that the ligand adopts different coordination mode to bond to tin atom in complexes **4**, **5** and **7**. As shown in Figs. 6 and 8, the ligand adopts mode **B** in complexes **4** and **5**, while it adopts mode **A** to bond to tin atom in complex **7** (see Fig. 10).

Furthermore, complex **4** is a dimer bridged by weak Sn···Cl intermolecular interactions between the two closest molecules. The Sn···Cl distance is 3.959 Å, just comparable to the sum of the van der Waals' radii of Sn and Cl (4.0 Å) [44]. The form of the dimer maybe the reason that the ligand adopts mode **B** to bond to tin atom in complex **4**. But the reason that the ligand adopts mode **B** to bond to tin atom in complex **5** is the large of stereo-constraint functions of phenyl groups and two dependent molecules. While complex **7** is a one-dimensional chain bridged by both intermolecular Sn···S and Sn···N contacts between the neighboring molecules. In which both the coordinated 2-sulfur atom and no-coordinated 3-nitrogen atom of the mpymt ligand bond to tin atom of neighboring molecules. The Sn···N distance (2.804 Å) is consistent with that of dibutyltin derivatives of 2-mercaptobenzoxazole [2.81(1) Å] [45], and still shorter than the sum of the van der Waals radii of tin and nitrogen (3.74 Å) [35]. The Sn···S distance (3.672 Å) lies within the sum of the van der waals radii of Sn and S (4.0 Å) [34]. Besides, the stereo-constraints of Cl– group is smaller than that of $PhCH_2$– group in complex **2**, which maybe benefit the coordination of 3-nitrogen atoms. All above information indicates that it is the stereo-constraints, intermolecular interactions and crystal packing requirements that lead the ligand to adopt different coordination modes to bond to tin in complexes **4**, **5** and **7**.

3.2.3. $Me_2Sn(SC_5H_5N_2)_2$ (**8**), $(n\text{-}Bu)_2Sn(SC_5H_5N_2)_2$ (**9**), $Ph_2Sn(SC_5H_5N_2)_2$ (**10**) and $(PhCH_2)_2Sn\text{-}(SC_5H_5N_2)_2$ (**11**)

Selected bond lengths and bond angles for **8**, **9**, **10** and **11** are given in Tables 9–12, respectively. The molecular structures of **8**, **9**, **10** and **11** are shown in Fig. 12–15, respectively.

For complex **8**, the tin atom is coordinated to two methyl groups and to two sulfur atoms from two deprotonated ligands (mpymt). The Sn–C distance 2.102(5) Å and the Sn–S distances [2.480(2) and 2.484(3) Å] are similar to those found in [$SnMe_2(Spym)_2$] [2.17(1)–2.25(1) and 2.466(4) Å, respectively] [46]. The Sn–S distances are close to the typical length of a single covalent bond. Due to the steric effect, the Sn–N distances [2.650(7) and 2.752(6) Å] are longer than those of complex **4**, so they can be regarded as weak intramolecular interactions, but they are shorter than those found in [$SnMe_2(Spym)_2$] (2.83(2) Å) [46]. The bite angles S(1)–Sn(1)–N(1), S(2)–Sn(1)–N(4) of complex **8** [60.28(18)° and 61.35(18)°, respectively] are reconcilable with skew-trapezoidal bipyramid geometry. This geometry can also be considered as a distorted *trans* regular octahedron. The S–C distances [1.773(9) and 1.782(15) Å] are consistent with single-bond character [47].

Table 9
Selected bond lengths and angles for the complex **8**

Bond	Distance (Å)	Bond	Distance (Å)
Sn(1)–C(11)#1	2.102(5)	Sn(1)–S(2)	2.484(3)
Sn(1)–C(11)	2.102(5)	Sn(1)–N(4)	2.650(7)
Sn(1)–S(1)	2.480(2)	Sn(1)–N(1)	2.752(6)
S(1)–C(1)	1.773(9)	S(2)–C(6)	1.782(15)
Angle	Amplitude (°)	Angle	Amplitude (°)
C(11)#1–Sn(1)–C(11)	127.0(3)	S(2)–Sn(1)–N(4)	61.35(18)
C(11)–Sn(1)–S(1)	107.95(12)	C(11)–Sn(1)–N(1)	82.71(13)
C(11)#1–Sn(1)–S(2)	109.23(12)	S(1)–Sn(1)–N(1)	60.28(18)
C(11)–Sn(1)–S(2)	109.23(12)	S(2)–Sn(1)–N(1)	148.9(2)
S(1)–Sn(1)–S(2)	88.64(9)	N(4)–Sn(1)–N(1)	149.7(2)
C(11)#1–Sn(1)–N(4)	83.93(12)	S(1)–Sn(1)–N(4)	149.99(16)
C(11)–Sn(1)–N(4)	83.93(12)		

Table 10
Selected bond lengths and angles for the complex **9**

Bond	Distance (Å)	Bond	Distance (Å)
Sn(1)–C(17)	2.115(5)	Sn(1)–N(3)	2.700(4)
Sn(1)–C(11)	2.124(4)	Sn(1)–N(1)	2.933(4)
Sn(1)–S(2)	2.4502(14)	S(1)–C(1)	1.762(5)
Sn(1)–S(1)	2.4753(15)	S(2)–C(6)	1.745(5)
Angle	Amplitude (°)	Angle	Amplitude (°)
C(17)–Sn(1)–C(11)	122.27(19)	S(2)–Sn(1)–N(3)	60.57(9)
C(17)–Sn(1)–S(2)	113.30(12)	S(1)–Sn(1)–N(3)	145.75(9)
C(11)–Sn(1)–S(2)	109.70(14)	C(17)–Sn(1)–N(1)	83.81(14)
C(17)–Sn(1)–S(1)	108.09(15)	C(11)–Sn(1)–N(1)	84.64(15)
C(11)–Sn(1)–S(1)	112.06(13)	S(2)–Sn(1)–N(1)	142.63(10)
S(2)–Sn(1)–S(1)	85.36(5)	S(1)–Sn(1)–N(1)	57.37(9)
C(17)–Sn(1)–N(3)	84.40(15)	N(3)–Sn(1)–N(1)	156.80(13)
C(11)–Sn(1)–N(3)	84.88(14)		

Table 11
Selected bond lengths and angles for the complex **10**

Bond	Distance (Å)	Bond	Distance (Å)
Sn(1)–C(11)	2.046(14)	Sn(1)–N(3)	2.782(10)
Sn(1)–C(15)	2.242(16)	Sn(1)–N(1)	2.889(11)
Sn(1)–S(1)	2.477(5)	S(1)–C(1)	1.749(9)
Sn(1)–S(2)	2.482(4)	S(2)–C(6)	1.759(12)
Angle	Amplitude (°)	Angle	Amplitude (°)
C(11)–Sn(1)–C(15)	131.7(7)	S(1)–Sn(1)–N(3)	144.9(2)
C(11)–Sn(1)–S(1)	111.3(4)	S(2)–Sn(1)–N(3)	59.3(2)
C(15)–Sn(1)–S(1)	104.8(6)	C(11)–Sn(1)–N(1)	85.1(5)
C(11)–Sn(1)–S(2)	109.1(4)	C(15)–Sn(1)–N(1)	86.9(5)
C(15)–Sn(1)–S(2)	104.5(6)	S(1)–Sn(1)–N(1)	59.2(2)
S(1)–Sn(1)–S(2)	85.80(15)	S(2)–Sn(1)–N(1)	145.0(2)
C(11)–Sn(1)–N(3)	85.8(5)	N(3)–Sn(1)–N(1)	155.6(3)
C(15)–Sn(1)–N(3)	82.4(5)		

The crystal structure of **8** shows ring-stacking interactions, each mpymt group is arranged face-to-face at distances of 4.161 and 4.227 Å, respectively; and show π–stacking interactions [46]. As shown in Fig. 12, steric requirements and π–π interactions maybe the reasons that lead the mpymt in complex **8** to adopt both the $N(1)/S^2$ and $S^2/N(3)$ coordination modes.

For three complexes **9**, **10** and **11**, compare to complex **8**, the mpymt ligand adopts only the remote linkage form **B**: $N(1)/S^2$ coordination mode, which is also attributed to

Table 12
Selected bond lengths and angles for the complex **11**

Bond	Distance (Å)	Bond	Distance (Å)
Sn(1)–C(11)	2.148(5)	Sn(1)–N(1)	2.583(4)
Sn(1)–C(18)	2.193(5)	Sn(1)–N(3)	2.752(5)
Sn(1)–S(1)	2.513(2)	S(1)–C(1)	1.760(5)
Sn(1)–S(2)	2.526(2)	S(2)–C(6)	1.745(5)
Angle	Amplitude (°)	Angle	Amplitude (°)
C(11)–Sn(1)–C(18)	137.24(19)	S(1)–Sn(1)–N(1)	61.53(10)
C(11)–Sn(1)–S(1)	109.96(16)	S(2)–Sn(1)–N(1)	148.12(9)
C(18)–Sn(1)–S(1)	106.51(15)	C(11)–Sn(1)–N(3)	81.31(19)
C(11)–Sn(1)–S(2)	105.06(15)	C(18)–Sn(1)–N(3)	80.77(17)
C(18)–Sn(1)–S(2)	98.56(13)	S(1)–Sn(1)–N(3)	146.10(10)
S(1)–Sn(1)–S(2)	86.59(9)	S(2)–Sn(1)–N(3)	59.51(11)
C(11)–Sn(1)–N(1)	87.33(18)	N(1)–Sn(1)–N(3)	152.38(13)
C(18)–Sn(1)–N(1)	91.01(16)		

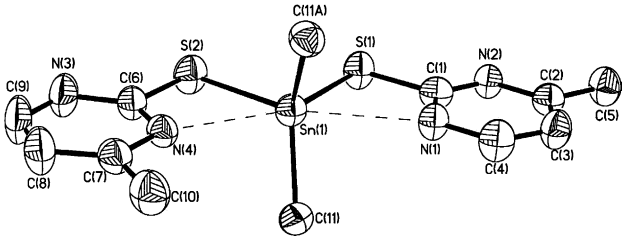

Fig. 12. Molecular structure of complex **8**.

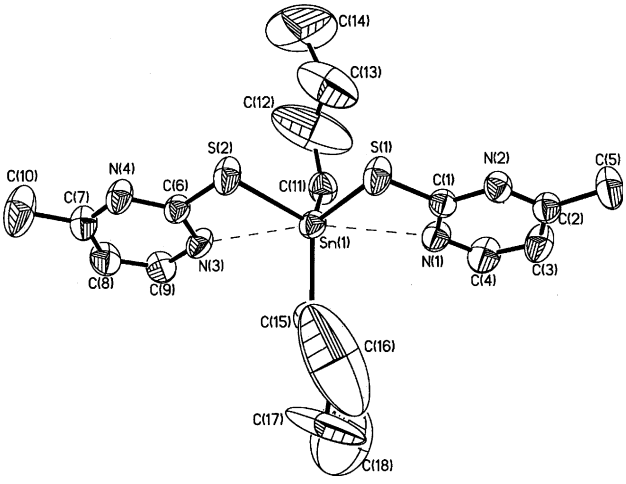

Fig. 13. Molecular structure of complex **9**.

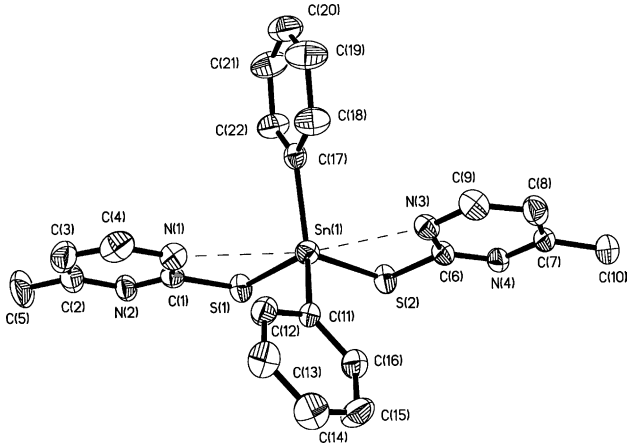

Fig. 14. Molecular structure of complex **10**.

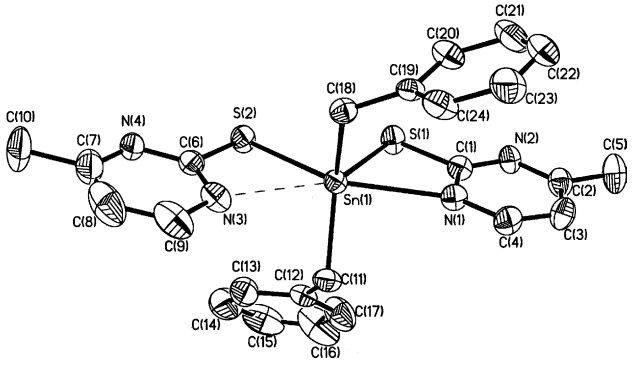

Fig. 15. Molecular structure of complex **11**.

the stereo-constraints. In each case, two carbons and two sulfur atoms are covalently linked to the metal. The valence extension is performed via the nitrogen atoms, N1 and N3 of the Hmpymt ligand. The two chelating sulfur occupy *cis* positions. The Sn–C distances [from 2.092(9) to 2.193(5) Å], are quite close to those found in $Bu_2Sn(mbo)_2$ [2.09(2) and 2.19(3) Å]. The Sn–S distances [2.466(3) and 2.474(3) Å for **9**, 2.4502(14) and 2.4753(15) Å for **10**, 2.513(2) and 2.526(2) Å for **11**, respectively] are similar to those found in other $[SnR_2(chelate)_2]$ systems [11,48,49]. Three complexes are different distinctly from each other with regard to their weak intramolecular Sn–N interactions [2.825(7) and 2.844(7) Å for **9**, 2.700(4) and 2.933(4) Å for **10**, 2.583(4) and 2.752(5) Å for **11**, respectively], they are all longer than the sum of the covalent radii of tin and

nitrogen atoms (2.15 Å), but still lie within the sum of the van der Waals radii of the two atoms (3.74 Å) [35]. The geometries of complexes **9**, **10** and **11** can also be considered as distorted *trans* regular octahedrons. The S–C distances [from 1.725(8) to 1.762(5) Å] are consistent with those found in complex **8**.

Besides, for complex **11**, similar to complex **7**, also contains one-dimensional chain bridged by weak Sn···S intermolecular interactions between the neighboring molecules. The Sn···S distance (3.774 Å), is consistent with that of complex **7** and also shorter than the sum of the van der waals radii of Sn and S (4.0 Å) [34].

4. Conclusions

In summary, the dominant isomer changes drastically in the mpymt system. The mode **B** is formed in complexes **2**, **4**, **5**, **9**, **10** and **11**, while the mode **A** is adopted in complexes **1**, **6** and **7**, respectively, both the mode **A** and mode **B** are adopted in complex **8**. These distinctions are thought to be due to a number of factors, such as steric requirements, inter and/or intra-molecular interactions, crystal packing requirements and so on [11]. For example, the conclusion is well consistent with the sequence of stereo-constraints, phenyl ≈ $PhCH_2$ > *n*-butyl > methyl > Cl [50]. When the larger the stereo-constraint of R groups exist, it is reasonable to consider that the 4–methyl group lies away from the R– groups to minimize the steric repulsion [51]. However, the main isomer is the adjacent form in complexes **1** irrespective of the steric hindrance. This fact indicates that an attractive interaction exists between the CH_3– group of the ligand and the Ph– group for complex **1**. Such an attractive interaction between an alkyl group and a π system is called a CH–π interaction and was first advocated by Nishio [52–54]. Thus, the drastic change in the main linkage isomer between complexes **1** and **2** is attributed to the existence of a CH–π interaction in the former complexes. Another support is given by above the ^1H NMR spectra.

5. Supplementary Material

Crystallographic data (excluding structure factors) for the structure reported in this paper (**1**, **2**, **4**, **7**, **8**, **9**, **10**, **11**) have been deposited with the Cambridge Crystallographic Data Center as supplementary publication no. CCDC-22795, 227963, 218578, 227964,218576, 227965, 227966, 228171, respectively. Copies of the data can be obtained free of charge on application to the Director, CCDC, 12 Union Road, Cambridge, CB2 1EZ, UK (Fax: +44 1223 336033; e-mail: deposit@ccdc.cam.ac.uk or www:http://www.ccdc.cam.ac.ck).

Acknowledgement

The authors thank the National Natural Science Foundation of China (20271025) and the Natural Science Foundation of Shandong Province for financial support.

References

[1] P.J. Smith (Ed.), Chemistry of Tin, second ed., Blackie, London, 1998.
[2] C.H. Yoder, L.A. Margolis, J.M. Horne, J. Organomet. Chem. 633 (2001) 33.
[3] V. Narayanan, M. Nasr, K.D. Paull, in: M. Gielen (Ed.), Tin-Based Anti-Tumor Drugs, Springer, Berlin, 1990, p. 201.
[4] W. Piver, T. Environ, Health Perspect. 4 (1973) 61.
[5] G.J.M. van de Kerk, in: J.J. Zuckerman (Ed.), Organotin Compounds, American Chemical Society, Washington, 1976, p. 1.
[6] J.A. Carbon, H. David, M.H. Studier, Science 161 (1968) 1146.
[7] A. Holly, I. Votruba, K. Jost, Coll. Czech Chem. Commun 39 (1974) 634.
[8] C.L. Ma, F. Li, D.Q. Wang, H.D. Yin, J. Organomet. Chem. 667 (2003) 5.
[9] C.L. Ma, Q. Jiang, R.F. Zhang, Appl. Organometal. Chem. 17 (2003) 623.
[10] C.L. Ma, Q. Jiang, R.F. Zhang, Polyhedron 23 (2004) 779.
[11] R.M. Fernandes, E.S. Lang, E.M.V. López, G.F. de Sousa, Polyhedron 21 (2002) 1149.
[12] K. Yamanari, K. Okusako, K. Kushi, S. Kaizaki, J. Chem. Soc., Dalton Trans. (1992) 1615.
[13] K. Yamanari, Y. Kushi, A. Fuyuhiro, S. Kaizaki, J. Chem. Soc., Dalton Trans. (1993) 403.
[14] K. Sisido, J. Am. Chem. Soc. 83 (1961) 538.
[15] J.R. May, W.R. Mc Whinnie, R.C. Pollerm, Spectrochim. Acta 27A (1971) 969.
[16] B.S. Sarawat, G. Srivastava, R.C. Mehrotra, Inorg. Chim. Acta 36 (1979) 289.
[17] S.G. Teoh, G.Y. Yeap, S.B. Teo, H.K. Fun, Polyhedron 14 (1995) 8.
[18] J.R. Durig, R. Layton, D.W. Sink, B.R. Mitchell, Spectrochim. Acta 21 (1965) 1367.
[19] R. Visalakshi, V.K. Jain, S.K. Kulshreshtha, G.S. Rao, Indian J. Chem. 28A (1989) 51.
[20] A. Tarassoli, A. Asadi, P.B. Hitchcock, J. Organomet. Chem. 645 (2002) 105.
[21] P.G. Sousa, R.M. Silva, A. Cesar, J.L. Wardell, J.C. Huffman, A. Abras, J. Organomet. Chem. 605 (2000) 82.
[22] T.P. Lockhart, W.F. Manders, Inorg. Chem. 25 (1986) 892.
[23] T.P. Lockhart, W.F. Manders, J.J. Zuckerman, J. Am. Chem. Soc. 107 (1985) 4546.
[24] J. Holecek, A. Lycka, Inorg. Chim. Acta 118 (1986) L15.
[25] J. Holecek, M. Nadvornik, K. Handlir, A. Lycka, J. Organomet. Chem. 315 (1986) 299.
[26] A. Tarassoli, T. Sedaghat, B. Neumüller, M. Ghassemzadeh, Inorg. Chim.Acta 318 (2001) 15.
[27] R. Colton, D. Dakternieks, Inorg. Chim. Acta 148 (1988) 31.
[28] K. Handlíř, A. Lyčka, J. Holeček, M. Nádvorník, V. Pejchal, A. Sebald, Collect. Czech. Chem. Commun. 59 (1994) 885.

[29] C. Pettinari, F. Marchetti, A. Gregori, A. Cingolani, J. Tanski, M. Rossi, F. Caruso, Inorg. Chim. Acta 257 (1997) 37.
[30] Z.H. Chohan, R.A. Howie, J.L. Wardell, J. Organomet. Chem. 577 (1999) 140.
[31] B. Wrackmeyer, Ann. Rep. NMR Spectrosc. 16 (1985) 73.
[32] J. Susperregui, M. Bayle, J.M. Leger, G. Deleris, J. Organomet. Chem. 556 (1998) 105.
[33] B.D. James, R.J. Magee, W.C. Patalinghug, B.W. Skelton, A.H. White, J. Organomet. Chem. 467 (1994) 51.
[34] J.S. Casas, A. Castineiras, E.G. Martinez, A.S. González, A. Sánchez, J. Sordo, Polyhedron 16 (1997) 795.
[35] J.E. Hubeey, E.A. Keiter, R.L. Keiter, Principles and Applications of Inorganic Chemistry, fourth ed., Harper Collins, New York, 1993.
[36] C.V.R. Moura, A.P.G. Sousa, R.M. Silva, A. Abras, M. Horner, A.J. Bortoluzzi, C.A.L. Filgueriras, J.L. Wardell, Polyhedron 18 (1999) 2961.
[37] B.H. Ye, X.M. Chen, G.Q. Xue, L.N. Ji, J. Chem. Soc. Dalton Trans. (1998) 2827.
[38] T. Steiner, B. Lutz, J. van der Maas, A.M.M. Kroon, M. Tamm, Chem. Commun. (1998) 171.
[39] M. Nishio, M. Hirota, Y. Umezawa, The CH–π interaction, Wiley-VCH, New York, 1998.
[40] A.R. Narga, M. Schuermann, C. Silvestru, J. Organomet. Chem. 623 (2001) 161.
[41] F.H. Allen, O. Kennard, D.G. Watson, L. Brammer, A.G. Orpen, R. Taylor, J. Chem. Soc. Perkin Trans. II (1987) S1.
[42] R.C. Poller, The Chemistry of Organotin Compounds, Logos Press, London, 1970, p. 227A.
[43] Z.H. Chohan, R.A. Wardell, J. Organometal. Chem. 577 (1999) 140.
[44] A. Bondi, J. Phys. Chem. 68 (1964) 441.
[45] J. Susperregui, M. Bayle, J. Léger M., G. Déléris, J. Organomet. Chem. 556 (1998) 105.
[46] S.K. Hadjikakou, M.A. Demertzis, M. Kubicki, D. Kovala-Demertzi, Appl. Organometal. Chem. 14 (2000) 727.
[47] R. Schmiedgen, F. Huber, H. Preut, G. Ruisi, R. Barbieri, Appl. Organomet. Chem. 8 (1994) 397.
[48] R. Schmiedgen, F. Huber, H. Preut, Acta Crystallogr. Sect. C 49 (1993) 1735.
[49] S.W. Ng, C. Wei, V.G. Kumar Das, T.C.W. Mak, J. Organomet. Chem. 334 (1987) 295.
[50] C.L. Ma, F. Li, Q. Jiang, R.F. Zhang, J. Organomet. Chem. 689 (2004) 69.
[51] K. Yamanari, K. Okusako, Y. Kushi, S. Kaizaki, J. Chem. Soc., Dalton Trans. (1992) 1621.
[52] M. Nishio, Kagaku No Ryoiki 31 (1977) 998.
[53] M. Nishio, M. Hirota, Tetrahedron 45 (1989) 7201.
[54] M. Nishio, Y. Umezawa, M. Hirota, Y. Takeuchi, Tetrahedron 51 (1995) 8665.